Piezo-phototronic Effect Enhanced Visible/UV Photodetector of a Carbon-Fiber/ZnO-CdS Double-Shell Microwire

Fang Zhang,[†,‡] Simiao Niu,[†] Wenxi Guo,[†] Guang Zhu,[†] Ying Liu,[†] Xiaoling Zhang,[‡] and Zhong Lin Wang[†,§,*]

[†]School of Material Science and Engineering, Georgia Institute of Technology, Atlanta, Georgia 30332-0245, United States, [‡]Key Laboratory of Cluster Science of Ministry of Education, School of Chemistry, Beijing Institute of Technology, Beijing 100081, China, and [§]Satellite Research Facility, MANA, International Center for Materials Nanoarchitectonics, National Institute for Materials Science, 1-1 Namiki, Tsukuba, 305-0044, Japan

ABSTRACT A branched ZnO-CdS double-shell NW array on the surface of a carbon fiber (CF/ZnO-CdS) was successfully synthesized *via* a facile two-step hydrothermal method. Based on a single CF/ZnO-CdS wire on a polymer substrate, a flexible photodetector was fabricated, which exhibited ultrahigh photon responsivity under illuminations of blue light (1.11×10^5 A/W, 8.99×10^{-8} W/cm^2, 480 nm), green light (3.83×10^4 A/W, 4.48×10^{-8} W/cm^2, 548 nm), and UV light (1.94×10^5 A/W, 1.59×10^{-8} W/cm^2, 372 nm), respectively. The responsivity of this broadband photon sensor was enhanced further by as much as 60% when the device was subjected to a −0.38% compressive strain. This is because the strain induced a piezopotential in ZnO, which tunes the barrier height at the ZnO−CdS heterojunction interface, leading to an optimized optoelectronic performance. This work demonstrates a promising application of piezo-phototronic effect in nanoheterojunction array based photon detectors.

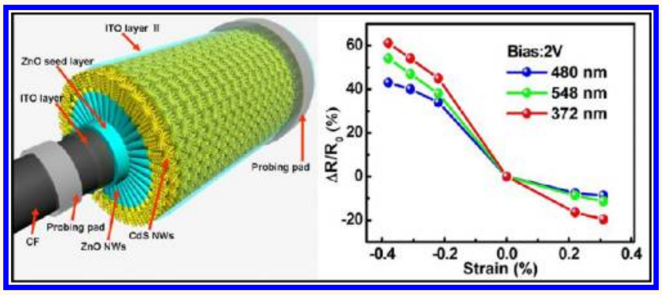

KEYWORDS: carbon fiber · branched ZnO-CdS double-shell nanowire · photodetector · piezopotential · piezo-phototronic effect

One-dimensional nanostructure arrays are of increasing attractiveness in various applications for their unique geometrical structures in providing a large surface-to-volume ratio, a direct pathway for charge transport, and low reflectance induced by light scattering and trapping.[1−3] For example, ZnO nanowire (NW) arrays have been widely used to fabricate electronic, optoelectronic, electrochemical, and electromechanical devices by taking advantage of their special semiconducting, photonic, and piezoelectric properties.[4−6] However, pure ZnO NWs cannot absorb wavelengths below the band gap, which in the UV range largely limits their wide spectral sensitivity for applications in photocatalysis, photovoltaics, and optoelectronics, such as broadband photodetection. Therefore, a composite structured ZnO NW array is desirable for fabrication of band gap engineered devices with good photoresponse in a wide wavelength region.

Herein we report a multiband visible/UV photodetector using the branched ZnO-CdS double-shell NW array on carbon fiber (CF/ZnO-CdS wire), which is a promising building block for several reasons beyond ZnO NW arrays. First, the tree-like chemical connection, with ZnO (<3.37 eV, 370 nm) NWs as the inner shell ("trunks") and CdS (<2.40 eV, 516 nm) NWs as the outer shell ("branches"), comprises a type-II heterostructure with a staggered alignment, which enables visible/UV broadband sensitivity and facilitates spatial charge separation by reducing the electron−hole pair recombination.[7,8] Second, the CdS NW array grown on ZnO wire provides an enlarged specific surface area for visible/UV light absorption as well as efficient channels for photogenerated electron transport, compared to the traditional CdS nanoparticle shell.[9,10] Moreover, the direct integration of branched ZnO-CdS double-shell NWs and carbon fiber

* Address correspondence to zlwang@gatech.edu.

Received for review March 11, 2013 and accepted April 16, 2013.

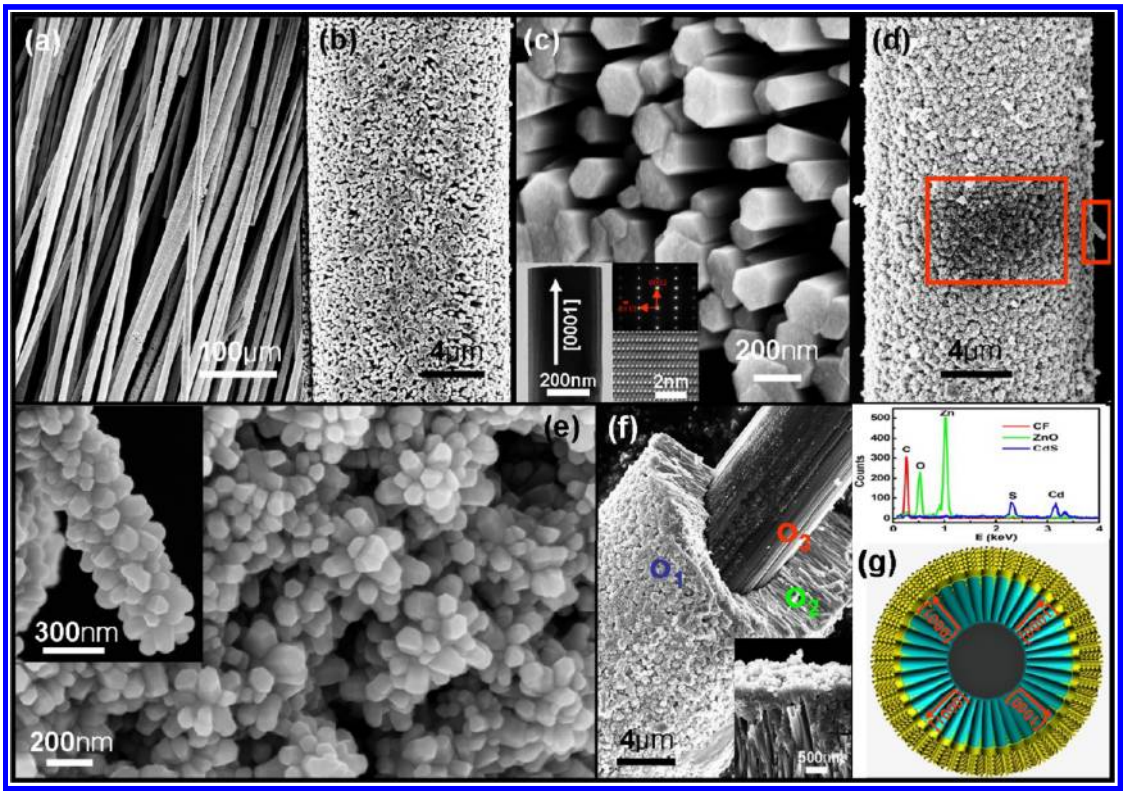

Figure 1. (a) Low-magnification SEM image of branched ZnO-CdS double-shell nanowire arrays on carbon fibers (CF/ZnO-CdS wires). (b, c) SEM images of a ZnO nanowire array on a carbon fiber at different magnifications. Inset in (c) shows TEM and HRTEM images and SAED pattern taken from a ZnO nanowire. (d) SEM image of a branched ZnO-CdS double-shell nanowire array on a carbon fiber. (e) Top view and side view SEM images of branched ZnO-CdS double-shell nanowires taken from the marked areas in (d). (f) Cross-sectional SEM image of a CF/ZnO-CdS wire. Inset shows the EDX elemental profiles of Cd, S, Zn, O, and C taken from the corresponding points. (g) Three-dimensional structure model of a CFB/ZnO-CdS wire showing the relationship between the CdS nanowire outer shell (yellow branches), the ZnO nanowire inner shell (blue trunks), and the carbon fiber core (dark substrate).

(CF) not only builds up a three-dimensional (3D) nanostructure array to effectively capture light from all directions but also introduces a flexible substrate with good conductivity and thermal stability.[11,12] Together, these advantages offer a new nanoheterostructure-based multiband photon sensor for broadband photodetection with ultrahigh photoresponsivity.

In addition, the piezo-phototronic effect can be used to largely enhance the performance of such a photon sensor. Since ZnO has a noncentral symmetric wurtzite structure, strain along the *c*-axis on the basic unit can cause a polarization, resulting in a piezopotential inside the crystal.[13−15] By utilizing the piezopotential created in the ZnO NW, the electron−hole pair generation, transport, separation, and/or recombination at the p/n junction of ZnO NW/p-polymer can be tuned and the efficiency of the hybridized inorganic/organic ultraviolet light-emitting diode is improved, which is referred to as the piezo-phototronic effect.[16] In our work, based on the unique configuration of branched ZnO-CdS double-shell NWs grown on CFs, photoresponsivity of the photodetector can be further enhanced by strain-induced piezopotential in the ZnO NW shell through modulating the barrier height at the ZnO−CdS heterojunction interface. This result provides a new method to optimize the performance of 3D multifunction NW arrays by introducing the piezo-phototronic effect.

RESULTS AND DISCUSSION

Figure 1a is a low-magnification scanning electron microscopy (SEM) image of CF/ZnO-CdS wires, showing that the CF substrates are uniformly and compactly covered by a ZnO-CdS double-shell NW array. Figure 1b and c are the SEM images of the dense ZnO NW array grown on a CF at different magnifications. As we can see, the ZnO NWs are hexagonal prismatic in shape with diameters of 100−300 nm and lengths of 4−5 μm. To further verify the crystalline structure, a high-resolution transmission electron microscopy (HRTEM) image and the corresponding select area electron diffraction (SAED) pattern were taken from the edge of a ZnO NW (the inset), indicating that the ZnO NWs are single crystalline with length direction along the *c*-axis ([0001]). Figure 1d displays a single CF/ZnO-CdS wire, and the magnified view of the marked areas (Figure 1e) shows the CdS NWs grown on the surface of the ZnO NW are also hexagonal prismatic in shape with diameters of 40−100 nm and lengths of 40−260 nm. Moreover, the cross section of a

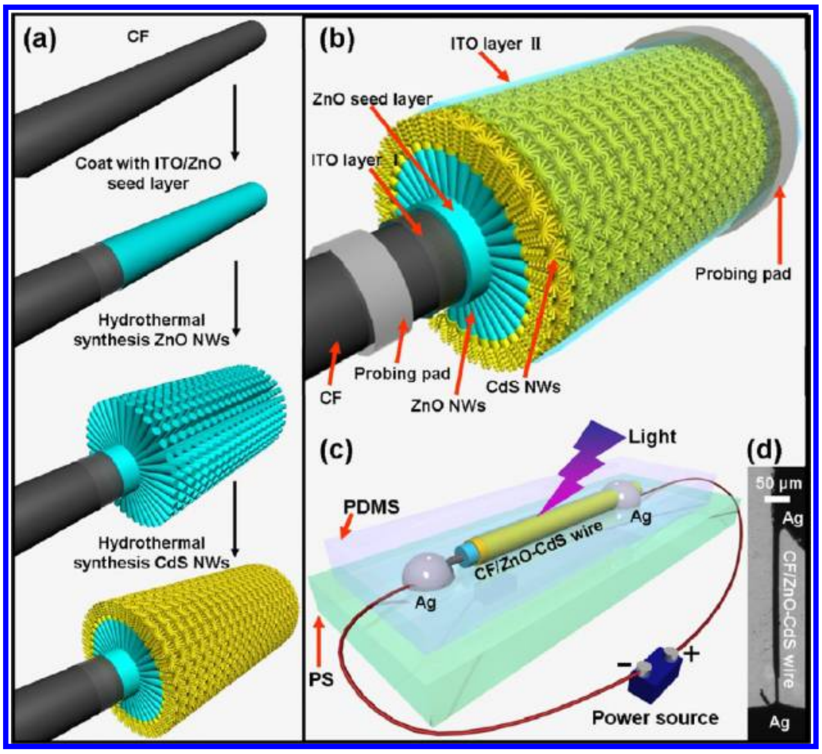

Figure 2. (a) Schematic diagram illustrating synthesis procedure of a branched ZnO-CdS double-shell nanowire array on a carbon fiber. (b, c) Schematic representation of the fabrication of a single CF/ZnO-CdS wire based photodetector. (d) Optical microscopy image of a typical device.

single CF/ZnO-CdS wire and energy dispersive X-ray (EDX) spectra from corresponding marked points are presented in Figure 1f, which clearly reveals that Cd and S are distributed in the outer shell (O_1), Zn and O are located in the inner shell (O_2), while C is located at the center (O_3). Thus, a three-dimensional (3D) schematic configuration of a single CF/ZnO-CdS wire is shown in Figure 1g, exhibiting the growth of a CdS NW array (yellow) on the upper part of the ZnO NW (blue) and the perpendicular orientation of such a branched ZnO-CdS double-shell NW array on the surface of the CF.

The branched ZnO-CdS double-shell NW array was grown on the CF *via* a two-step hydrothermal method, as displayed in Figure 2a. From the top to the bottom, the CF (black) was first coated with an ITO layer I (transparent) and a ZnO seed layer (blue) in sequence for a better adherence and conductivity; then, the ZnO NW array (blue) with very high density was grown perpendicularly on the surface of the CF by hydrothermal treatment; finally, the CdS NW array (yellow) was grown on the upper part of the ZnO NWs. Followed by top transparent contact deposition, a photon sensitive device can be built with the CF as source electrode and ITO layer II as drain electrode, as demonstrated in Figure 2b. Figure 2c presents the photodetector fabricated in our experiments: two electrodes of a single CF/ZnO-CdS/ITO wire were fixed on a PS substrate (typical length of ~3 cm, width of ~1 cm, and thickness of 0.5 mm) tightly by silver pastes; then a thin layer of polydimethylsiloxane (PDMS) was employed to package the device and make it optically transparent, flexible, and robust under repeated mechanical strains.[17,18] An optical microscope image of an as-fabricated device is shown in Figure 2d.

The performance of a single CF/ZnO-CdS wire (~236.7 μm in length and ~12.3 μm in diameter) based photodetector (device #1) under blue light (λ = 480 nm) illumination is summarized in Figure 3. Figure 3a shows typical I−V characteristics of a single CF/ZnO-CdS wire in the dark and under illumination at different intensities from 8.99×10^{-8} to 7.19×10^{-4} W/cm^2. Significantly, the absolute current increased from 3.91 μA (dark current) to 4.20 μA (8.99×10^{-8} W/cm^2) and further to 12.9 μA (7.19×10^{-4} W/cm^2) at an applied voltage of 2.0 V. Figure 3b illustrates the measured current response of a single CF/ZnO-CdS wire based photodetector under 480 nm light illumination at a bias of 2.0 V. With the light irradiation off and on, the current of the device rose very sharply from one state to another state with a response speed faster than 0.2 s. The intensity dependences of photocurrents ($I_{light} - I_{dark}$) are also plotted in Figure 3c. The photocurrent increased with the optical power and showed no saturation at high power intensity, offering a large dynamic range from 10^{-7} to 10^{-3} W/cm^2. Accordingly, the excellent photocurrent generation, good reproducibility, and fast response speed indicate that the developed CF/ZnO-CdS wire is a great candidate for applications in photon detection.

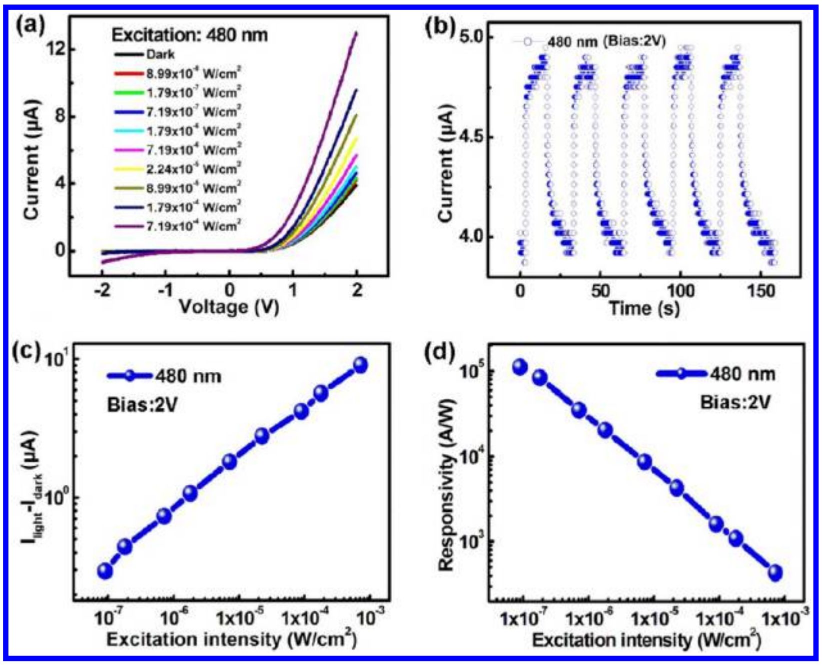

Figure 3. (a) Typical $I-V$ characteristics of single CF/ZnO-CdS wire based device, excited by blue light centered at 480 nm. (b) Repeatable response of a single CF/ZnO-CdS wire based device, excited by blue light centered at 480 nm. (c) Absolute photocurrent of a single CF/ZnO-CdS wire based device measured as a function of the excitation intensity. (d) Derived photon responsivity relative to excitation intensity on the CF/ZnO-CdS wire.

Moreover, as a critical parameter to determine the capability of a photodetector,[19] the total responsivity of the photodetector R is defined as

$$R = \frac{I_{\text{light}} - I_{\text{dark}}}{P_{\text{ill}}} = \frac{\eta_{\text{ext}} q}{h\nu} \Gamma_G \qquad (1)$$

$$P_{\text{ill}} = I_{\text{ill}} \times d \times l \qquad (2)$$

where I_{light}, I_{dark}, P_{ill}, η_{ext}, q, h, v, Γ_G, I_{ill}, d, and l are the current of the photodetector under illumination, the current of the photodetector in the dark, illumination power on the photodetector, external quantum efficiency (EQE), electronic charge, Planck's constant, frequency of the incident light, internal gain, excitation power, diameter of the CF/ZnO-CdS wire, and spacing between two silver pads, respectively. Remarkably, the calculated responsivity R of the present device is approximately 1.11×10^5 A/W at an intensity of 8.99×10^{-8} W/cm^2 under blue light illumination, corresponding to an EQE of $\sim 2.87 \times 10^7$ % if the internal gain Γ_G is assumed to be 1. These impressive values indicate, as for a visible/UV light sensor, the present device based on single CF/ZnO-CdS wire exhibits ultrahigh responsivity R and EQE as well as wide spectral sensitivity (1.11×10^5 A/W, 2.87×10^7 %, 480 nm, at 2 V bias), compared with the reported individual ZnSe-nanobelt-based blue/UV-light sensor (0.12 A/W, 37.2%, 400 nm, at 30 V bias).[20] Moreover, the achieved photoresponsivity also prevails over other broadband photodetectors based on semiconductor nanoheterojunctions, demonstrating to be $\sim 10^7$ times higher than a Si/ZnO core–shell NW array (1.0×10^{-2} A/W, 2%, 480 nm, −1 V) and $\sim 10^5$ times higher than the Si/CdS core–shell NW network (<1 A/W, <100%, 480 nm, −1 V).[21,22] The decrease of the responsivity at high light intensities could be attributed to the hole-trapping saturation, as has been observed from a ZnO nanowire based UV light photodetector.[17]

In addition, the single CF/ZnO-CdS wire based photodetector also exhibits excellent response to green and UV light, as indicated in Figures S1 and S2 in the Supporting Information. Surprisingly, the measured responsivity R (1.87×10^4 A/W) increased remarkably by 1.70×10^3 times when the device is illuminated with green light (548 nm, 1.79×10^{-7} W/cm^2, at 2 V bias), compared with a single ZnO-CdS core–shell NW device (11 A/W). Similarly, a great enhancement of 2.50×10^3 times (1.94×10^5 A/W/77.6 A/W) was also recorded under UV light illumination (372 nm, 1.59×10^{-8} W/cm^2, at 2 V bias).[23] These improvements are probably due to the unique configuration of the device, including the parallel connection of a large number of branched ZnO-CdS NWs with short length (4–5 μm) as well as the relatively large surface area of source (CF) and drain (ITO) electrodes, which can promote the efficiency of photoelectron generation/transport and decrease the opportunity for electron–hole recombination. Consequently, the performance of the CF/ZnO-CdS wire photodetector is significantly optimized by combining the 3D arrangement of a branched ZnO-CdS double-shell NW array with CF, which enables broadband detection with greatly enhanced flexibility, stability, and responsivity.

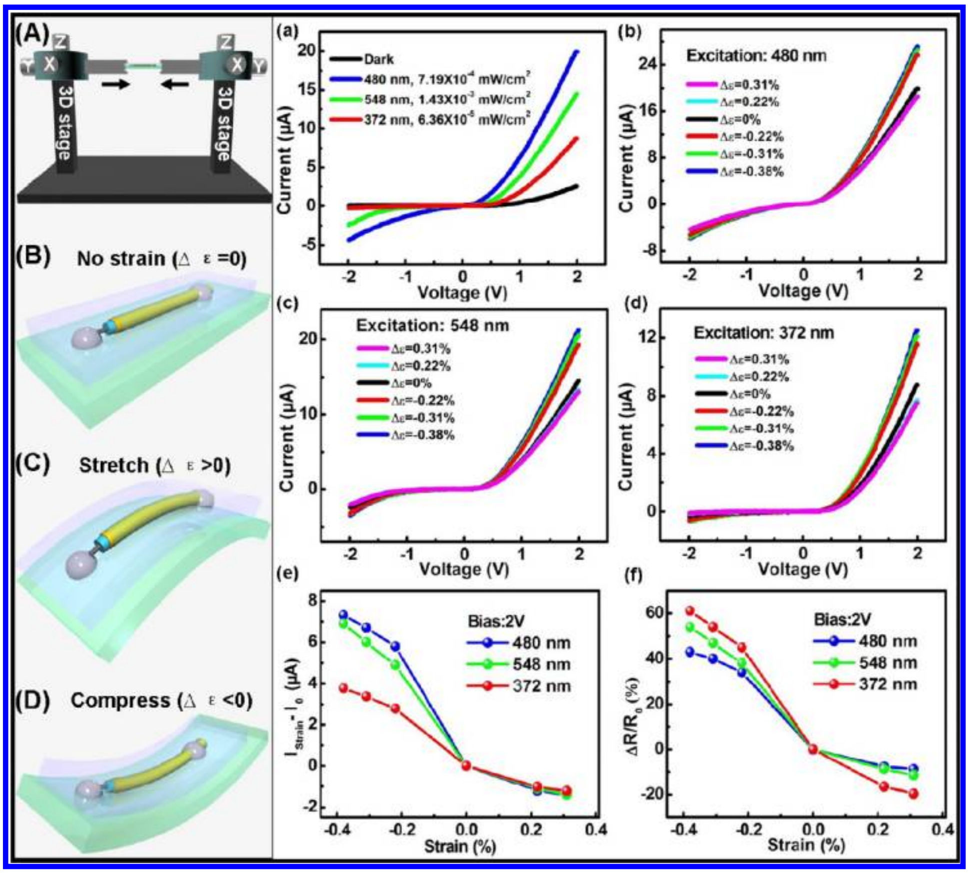

Figure 4. (A–D) Schematics of the measurement setup for studying the piezo-phototronic effect and the device under various strain conditions. (a–d) Typical *I*–*V* characteristics of a single CF/ZnO-CdS wire based device under different tensile and compressive strains, excited by blue light centered at 480 nm, green light centered at 548 nm, and UV light centered at 372 nm, respectively. (e, f) Changes of photocurrent and responsivity derived from (a–d); R_0 is set as responsivity under zero strain.

To further optimize the photoresponse of a single CF/ZnO-CdS wire using the effects of the piezoelectric field formed inside ZnO NWs, the photodetector (device #2) was subjected to different strains, as shown in Figure 4. Figure 4A demonstrates a schematic diagram of the measurement setup for studying the piezo-phototronic effect on the photodetector. With the ends of the PS substrate fixed on manipulation holders, two 3D mechanical stages with a movement resolution of 1 μm were used to apply a force to the PS substrate, introducing compressive or tensile strain that can be calculated according to Yang *et al.*'s work.[24] Figure 4B–D are corresponding schematic diagrams of the device under different strains.

The performances of the device in the dark and under illuminations of three different wavelengths are presented in Figure 4a. The piezo-phototronic effects on the device under blue, green, and UV light illuminations are illustrated respectively in Figure 4b–d. As can be seen in Figure 4b, with the tensile strain applied to the device increasing from 0%, to 0.22%, to 0.31%, the current at 2 V bias dropped step by step from 19.9, to 18.7, to 18.5 μA to nearly 7%, while with the compressive strain increasing from −0.22%, to −0.31%, to −0.38%, the corresponding current rose step by step from 25.6, to 26.6, to 27.1 μA to nearly 36.2%. A similar tendency was also observed under the illumination of green light or UV light, as exhibited in Figure 4c and d. As a result of the fluctuation of the output current, the photoresponse of the device was closely associated with the strain. Because the variation of dark current was negligible, the photocurrent changes at a fixed bias of 2 V under different strains were extracted from Figure 4a–d, plotted in Figure 4e correspondingly, which demonstrates clearly that compressive strain leads to a monotonic increase in current and tensile strain induces a monotonically decreasing current. As dominated by the enhancement of the photocurrent, the responsivity of this photodetector increased about 40–60% under a −0.38% compressive strain and decreased about 8–20% under a 0.31% tensile strain, as shown in Figure 4f. The enhanced performance of the photodetector under compressive strains is suggested to arise from the effective decrease of the barrier height between ZnO and CdS at the heterojunction interface due to the band modification caused by piezoelectric polarization charges, as discussed below.

A theoretical model is proposed to explain the piezophototronic effect on the performance of the

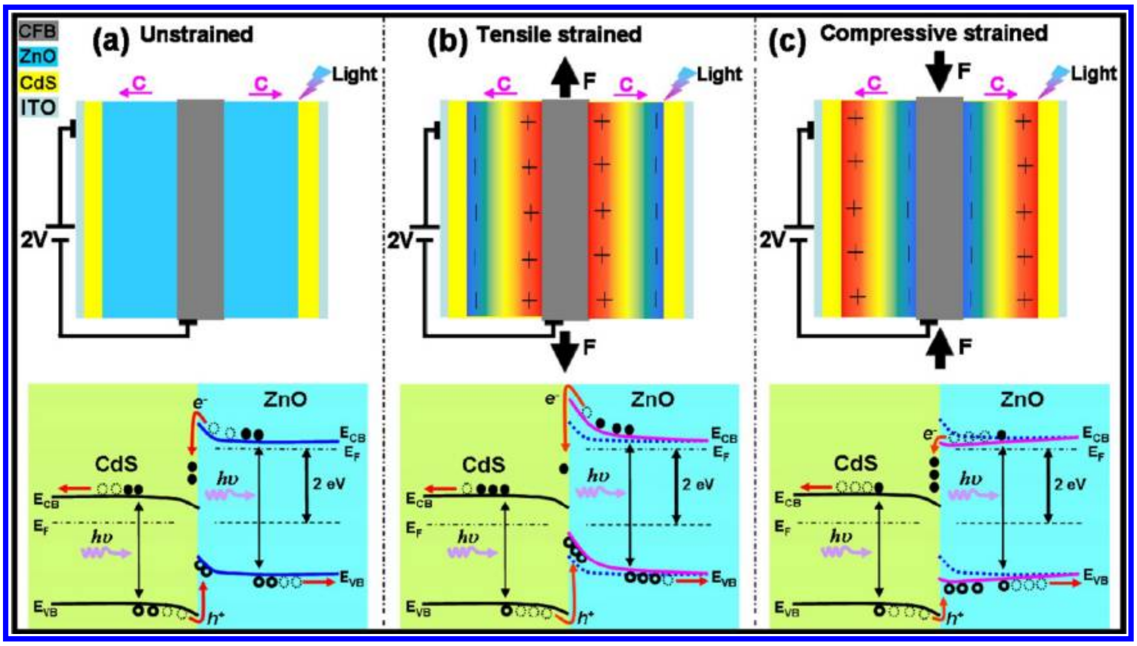

Figure 5. Schematics and energy band diagrams demonstrate the piezo-phototronic effect on a single CF/ZnO-CdS wire based device. (a) Schematic and the corresponding energy band diagram of a strain-free single CF/ZnO-CdS wire based device. (b) Piezopotential distribution and the corresponding energy band diagram of a single CF/ZnO-CdS wire based device under tensile strain. (c) Piezopotential distribution and the corresponding energy band diagram of a single CF/ZnO-CdS wire based device under compressive strain.

single CF/ZnO-CdS wire based photodetector, as shown in Figure 5. As the resistance is ignored for the ideal case, the energy band of ZnO shifts up by ~2 eV when the bias is applied on the heterojunction region of ZnO-CdS.[25,26] Figure 5a shows a schematic structure and corresponding energy band diagram of an unstrained device. Due to the sandwich structure of the device, tension along the CF/ZnO-CdS wire creates a compressive strain in alignment with ZnO NWs. With an assumption of low-doping in ZnO for simplicity, a piezopotential drop of approximately $V^+ - V^- = P_X L$ can be induced along the length of ZnO NWs (where P_X is axial polarization and L is the length of the ZnO NW). As well-illustrated in our previous works, with the *c*-axis ([0001]) of the ZnO NW positioned toward the outside, the piezopotential at the outer and inner ends of the ZnO NWs can be qualitatively described as V^- and V^+, which are of the same magnitude but opposite in sign (see Figure 5b).[27−30] Thus the local negative piezoelectric charges at the ZnO−CdS interface will lift up the conduction and valence bands of ZnO, resulting in an increase of the barrier height at the heterojunction interface.[31] Since electron−hole pairs can be generated in both ZnO (~3.3 eV) and CdS (~2.4 eV) under UV light (~3.34 eV, 372 nm) illumination, the increased barrier height will reduce the possibility of photogenerated electron transport from excited ZnO and accelerate the trapping of photogenerated holes from excited CdS at the ZnO−CdS interface.[32] As a result, the photocurrent and responsivity of the device are decreased with an increase in the applied tensile strain on the device.

In contrast, when a compression along the CF/ZnO-CdS wire leads to a tensile strain along the ZnO NWs, the piezopotential at the outer and inner ends of ZnO NWs can be qualitatively described as V^+ and V^-, respectively, as shown in Figure 5c. The effect of the local positive piezopotential at the ZnO−CdS interface will lower the conduction and valence bands of ZnO and result in a decrease of the barrier height at the heterojunction interface, which facilitates the transport of photogenerated electrons from excited ZnO and releases the trapping of photogenerated holes from excited CdS at the ZnO−CdS interface, thus enhancing the performance of the device. This is the basic mechanism of how the piezo-phototronic effect tunes the photoresponse of our single CF/ZnO-CdS wire based photodetector.

In the case of visible light illumination (for example ~2.59 eV, 480 nm), photogenerated electrons cannot be efficiently excited in ZnO (~3.3 eV), while the trapping effect still influences considerably the transport of photogenerated holes from the CdS side (~2.4 eV), resulting in an apparent enhancement/drop of responsivity, which is well consistent with the experimental results displayed in Figure 4f.[33]

CONCLUSIONS

In summary, we first fabricated a novel CF/ZnO-CdS microwire with a branched ZnO-CdS double-shell NW array grown on the surface of a CF. On the basis of a single CF/ZnO-CdS wire, we developed a photodetector exhibiting an excellent response on visible/UV light (372−548 nm). The responsivity of the CF/ZnO-CdS wire photodetector is nearly 10^6 times (1.11×10^5 A/W, 480 nm, at 2 V bias) higher than that of a ZnSe-nanobelt-based blue/UV-light sensor (0.12 A/W, 400 nm, at 30 V bias) and more than 10^3 times higher than that of a single ZnO-CdS core−shell NW based device. Moreover, using the piezo-phototronic effect, the performance of the CF/ZnO-CdS wire photodetector can be further enhanced by 60% when the device is subjected to a −0.38% compressive strain. This investigation demonstrates that the CF/ZnO-CdS wire has a potential for enhanced broadband photodetection with ultrahigh photoresponsivity.

EXPERIMENTAL SECTION

CF/ZnO-CdS wires were synthesized *via* a three-step process. First, a 200 nm thick ITO layer and a 100 nm thick ZnO seed layer were sequentially grown on the surface of a CF. Then, a ZnO NW array was grown on the CF with a nutrient solution, composed of an equal molar aqueous solution of $Zn(NO_3)_2 \cdot 6H_2O$ (0.05 M) and hexamethylenetetramine, in a mechanical convection oven (model Yamato DKN400, Santa Clara, CA, USA) at 85 °C for 8 h.[34] Finally, the CdS NW array was grown on the upper part of ZnO NWs by a hydrothermal method as described in our previous work: 1 mmol of cadmium nitrate ($Cd(NO_3)_2 \cdot 4H_2O$) and 3 mmol of thiourea (CH_4N_2S) were added to a given amount (80 mL) of distilled water; the ZnO NW coated CF was subsequently added to the resultant solution, and the mixture was transferred into a Teflon-lined stainless autoclave (25 mL capacity); the autoclave was sealed and maintained at 200 °C for 12 h; after the system cooled, the product was collected and vacuum-dried.[23] Detailed microscopic structures of the final branched ZnO-CdS double-shell NW array on CF were characterized by SEM [LEO 1550 at 7 kV] and TEM [JEOL 4000EX at 400 kV, TF30 at 300 kV].

The photodetector was excited by monochromatic blue light (centered at 480 nm), green light (centered at 548 nm), and UV light (centered at 372 nm) with a Nikon Intensilight C-HGFIE lamp as the source. The optical power density illuminated on the device was varied by means of neutral density filters and determined by a thermopile power meter (Newport 818P-001-12). *I*−*V* characteristics of the device were recorded by a Keithley 487 picoammeter/voltage source in conjunction with a GPIB controller (GPIB-USB-HS, NI 488.2).

Conflict of Interest: The authors declare no competing financial interest.

Acknowledgment. Research was supported by the Airforce, MURI, U.S. Department of Energy, Office of Basic Energy Sciences (DE-FG02-07ER46394), NSF, MANA, the World Premier International Research Center Initiative (WPI Initiative), MEXT, Japan, through a satellite lab at Georgia Tech, National Nature Science Foundation of China (No. 21275018), and the 111 Project in China (B07012). Thanks are extended to Jianjun Chen, Caofeng Pan, Yong Ding, and Sihong Wang for technical assistance.

Supporting Information Available: (1) Performance of a single CF/ZnO-CdS wire based photodetector under illumination of green light centered at 548 nm. (2) Performance of a single CF/ZnO-CdS wire based photodetector under illumination of UV light centered at 372 nm. This material is available free of charge *via* the Internet at http://pubs.acs.org.

REFERENCES AND NOTES

1. Tang, Y. B.; Chen, Z. H.; Song, H. S.; Lee, C. S.; Cong, H. T.; Cheng, H. M.; Zhang, W. J.; Bello, I.; Lee, S. T. Vertically Aligned p-Type Single-Crystalline GaN Nanorod Arrays on n-Type Si for Heterojunction Photovoltaic Cells. *Nano Lett.* **2008**, *8*, 4191–4195.
2. Mor, G. K.; Shankar, K.; Paulose, M.; Varghese, O. K.; Grimes, C. A. Use of Highly-Ordered TiO_2 Nanotube Arrays in Dye-Sensitized Solar Cells. *Nano Lett.* **2006**, *6*, 215–218.
3. Muskens, O. L.; Rivas, J. G.; Algra, R. E.; Bakkers, E. P. A. M.; Lagendijk, A. Design of Light Scattering in Nanowire Materials for Photovoltaic Applications. *Nano Lett.* **2008**, *8*, 2638–2642.
4. Lieber, C. M.; Wang, Z. L. Functional Nanowires. *MRS Bull.* **2007**, *32*, 99–104.
5. Wang, Z. L. From Nanogenerators to Piezotronics—A Decade-Long Study of ZnO Nanostructures. *MRS Bull.* **2012**, *09*, 814–827.
6. Wang, Z. L. Self-Powered Nanosensors and Nanosystems. *Adv. Mater.* **2012**, *24*, 280–285.
7. Tak, Y.; Hong, S. J.; Leeb, J. S.; Yong, K. Fabrication of ZnO/CdS Core/Shell Nanowire Arrays for Efficient Solar Energy Conversion. *J. Mater. Chem.* **2009**, *19*, 5945–5951.
8. Tak, Y.; Kim, H.; Lee, D.; Yong, K. Type-II CdS Nanoparticle-ZnO Nanowire Heterostructure Arrays Fabricated by a Solution Process: Enhanced Photocatalytic Activity. *Chem. Commun.* **2008**, 4585–4587.
9. Heo, K.; Lee, H.; Park, Y.; Park, J.; Lim, H. J.; Yoon, D.; Lee, C.; Kim, M.; Cheong, H.; Park, J.; *et al.* Aligned Networks of Cadmium Sulfide Nanowires for Highly Flexible Photodetectorswith Improved Photoconductive Responses. *J. Mater. Chem.* **2012**, *22*, 2173–2179.
10. Xu, F.; Yuan, Y. F.; Han, H. J.; Wu, D. P.; Gao, Z. Y.; Jiang, K. Synthesis of ZnO/CdS Hierarchical Heterostructure with Enhanced Photocatalytic Efficiency under Nature Sunlight. *CrystEngComm* **2012**, *14*, 3615–3622.
11. Guo, W. X.; Xu, C.; Wang, X.; Wang, S. H.; Pan, C. F.; Lin, C. J.; Wang, Z. L. Rectangular Bunched Rutile TiO_2 Nanorod Arrays Grown on Carbon Fiber for Dye-Sensitized Solar Cells. *J. Am. Chem. Soc.* **2012**, *134*, 4437–4441.
12. Fu, Y. P.; Lv, Z. B.; Hou, S. C.; Wu, H. W.; Wang, D.; Zhang, C.; Chu, Z. Z.; Cai, X.; Fan, X.; Wang, Z. L.; *et al.* Conjunction of Fiber Solar Cells with Groovy Micro-Reflectors as Highly Efficient Energy Harvesters. *Energy Environ. Sci.* **2011**, *4*, 3379–3383.
13. Wang, Z. L.; Song, J. H. Piezoelectric Nanogenerators Based on Zinc Oxide Nanowire Arrays. *Science* **2006**, *312*, 242–246.
14. Wang, Z. L. Piezotronic and Piezophototronic Effects. *J. Phys. Chem. Lett.* **2010**, *1*, 1388–1393.
15. Wang, Z. L. Progress in Piezotronics and Piezo-Phototronics. *Adv. Mater.* **2012**, *24*, 4632–4646.
16. Yang, Q.; Liu, Y.; Pan, C. F.; Chen, J.; Wen, X. N.; Wang, Z. L. Largely Enhanced Efficiency in ZnO Nanowire/p-Polymer Hybridized Inorganic/Organic Ultraviolet Light-Emitting Diode by Piezo-Phototronic Effect. *Nano Lett.* **2013**, *13*, 607–613.
17. Yang, Q.; Guo, X.; Wang, W.; Zhang, Y.; Xu, S.; Lien, D. H.; Wang, Z. L. Enhancing Sensitivity of a Single ZnO Micro-/Nanowire Photodetector by Piezo-Phototronic Effect. *ACS Nano* **2010**, *4*, 6285–6291.
18. Liu, Y.; Yang, Q.; Zhang, Y.; Yang, Z. Y.; Wang, Z. L. Nanowire Piezo-Phototronic Photodetector: Theory and Experimental Design. *Adv. Mater.* **2012**, *24*, 1410–1417.
19. Konstantatos, G.; Sargent, E. H. Nanostructured Materials for Photon Detection. *Nat. Nanotechnol.* **2010**, *5*, 391–400.
20. Fang, X. S.; Xiong, S. L.; Zhai, T. Y.; Bando, Y.; Liao, M. Y.; Gautam, U. K.; Koide, Y. S.; Zhang, X. G.; Qian, Y. T.; Golberg, D. High-Performance Blue/Ultraviolet-Light-Sensitive ZnSe-Nanobelt Photodetectors. *Adv. Mater.* **2009**, *21*, 5016–5021.
21. Sun, K.; Jing, Y.; Park, N.; Li, C.; Bando, Y.; Wang, D. L. Solution Synthesis of Large-Scale, High-Sensitivity ZnO/Si Hierarchical Nanoheterostructure Photodetectors. *J. Am. Chem. Soc.* **2010**, *132*, 15465–15467.
22. Manna, S.; Das, S.; Mondal, S. P.; Singha, R.; Ray, S. K. High Efficiency Si/CdS Radial Nanowire Heterojunction Photodetectors Using Etched Si Nanowire Templates. *J. Phys. Chem. C* **2012**, *116*, 7126–7133.

23. Zhang, F.; Ding, Y.; Zhang, Y.; Zhang, X. L.; Wang, Z. L. Piezo-Phototronic Effect Enhanced Visible and Ultraviolet Photodetection Using a ZnO-CdS Core-Shell Micro/Nanowire. *ACS Nano* **2012**, *6*, 9229–9236.
24. Yang, R. S.; Qin, Y.; Dai, L. M.; Wang, Z. L. Power Generation with Laterally Packaged Piezoelectric Fine Wires. *Nat. Nanotechnol.* **2009**, *4*, 34–39.
25. Xu, Y.; Schoonen, M. M. A. The Absolute Energy Positions of Conduction and Valence Bands of Selected Semiconducting Minerals. *Am. Mineral.* **2000**, *85*, 543–556.
26. Xu, F.; Volkov, V.; Zhu, Y.; Bai, H. Y.; Rea, A.; Valappil, N. V.; Su, W.; Gao, X. Y.; Kuskovsky, I. L.; Matsui, H. Long Electron-Hole Separation of ZnO-CdS Core-Shell Quantum Dots. *J. Phys. Chem. C* **2009**, *113*, 19419–19423.
27. Li, Z. T.; Wang, Z. L. Air/Liquid-Pressure and Heartbeat-Driven Flexible Fiber Nanogenerators as a Micro/Nano-Power Source or Diagnostic Sensor. *Adv. Mater.* **2011**, *23*, 84–89.
28. Pan, C. F.; Li, Z. T.; Guo, W. X.; Zhu, J.; Wang, Z. L. Fiber-Based Hybrid Nanogenerators for/as Self-Powered Systems in Biological Liquid. *Angew. Chem., Int. Ed.* **2011**, *50*, 1–6.
29. Bae, J.; Park, Y. J.; Lee, M.; Cha, S. N.; Choi, Y. J.; Lee, C. S.; Kim, J. M.; Wang, Z. L. Single-Fiber-Based Hybridization of Energy Converters and Storage Units Using Graphene as Electrodes. *Adv. Mater.* **2011**, *23*, 3446–3449.
30. Lee, M.; Chen, C. Y.; Wang, S. H.; Cha, S. N.; Park, Y. J.; Kim, J. M.; Chou, L. J.; Wang, Z. L. A Hybrid Piezoelectric Structure for Wearable Nanogenerators. *Adv. Mater.* **2012**, *24*, 1759–21764.
31. Pan, C. F.; Niu, S. M.; Ding, Y.; Dong, L.; Yu, R. M.; Liu, Y.; Zhu, G.; Wang, Z. L. Enhanced Cu_2S/CdS Coaxial Nanowire Solar Cells by Piezo-Phototronic Effect. *Nano Lett.* **2012**, *12*, 3302–3307.
32. Shen, Q. M.; Zhao, X. M.; Zhou, S. W.; Hou, W. H.; Zhu, J. J. ZnO/CdS Hierarchical Nanospheres for Photoelectrochemical Sensing of Cu^{2+}. *J. Phys. Chem. C* **2011**, *115*, 17958–17964.
33. Tak, Y.; Kim, H.; Lee, D.; Yong, K. Type-II CdS Nanoparticle−ZnO Nanowire Heterostructure Arrays Fabricated by a Solution Process: Enhanced Photocatalytic Activity. *Chem. Commun.* **2008**, 4585–4587.
34. Xu, S.; Lao, C. S.; Weintraub, B.; Wang, Z. L. Density-Controlled Growth of Aligned ZnO Nanowire Arrays by Seedless Chemical Approach on Smooth Surfaces. *J. Mater. Res.* **2008**, *23*, 2072–2077.